

## RESEARCH PAPER

# Experimental Data of Muon Hodoscope URAGAN for Investigations of Geoeffective Processes in the Heliosphere

Anna Kovylyayeva, Ivan Astapov, Anna Dmitrieva, Vladimir Borog, Natalia Osetrova and Igor Yashin

National Research Nuclear University MEPhI (Moscow Engineering Physics Institute), RU

Corresponding author: Anna Kovylyayeva (AAKovylyayeva@mephi.ru)

Muon hodoscope URAGAN continuously detects the angular distribution of muons in a wide range of zenith angles and allows one to obtain information about variations, both in the intensity and in angular characteristics of the muon flux, caused by active processes in the heliosphere, the magnetosphere and atmosphere of the Earth. Various parameters of the muon flux anisotropy and methods of calculation of these parameters are discussed. Real-time processing of a continuous flow of multidimensional data from the muon hodoscope URAGAN is quite a challenge. In the article, methods of formation and primary analysis of the data, their processing in real time and obtaining time series of various parameters of integral counting rate and angular anisotropy of the muon flux, which are important for the physical analysis of modulation processes of cosmic rays in the heliosphere, are presented.

**Keywords:** muons; barometric effect; temperature effect; muon hodoscope URAGAN; vector of local anisotropy; vector of relative anisotropy; coronal mass ejections

## Introduction

Secondary muons are generated in interactions of primary cosmic rays (CR) with nuclei of atoms of the atmosphere and keep quite well the directions of parent particles. Therefore, variations of primary CR caused by various phenomena associated with solar activity may be studied on the basis of the analysis of variations of the angular distribution of the muon flux measured in a real-time mode. This approach is the basis of the method of muon diagnostics developed in the Moscow Engineering Physics Institute using a specially designed muon hodoscope URAGAN (Shutenko et al. 2009; Astapov et al. 2013). Objects of the muon diagnostics are processes in the heliosphere of solar origin, which may cause negative influence on the vital activity of people (transpolar flights, orbital and interplanetary missions, and others). For implementation of the muon diagnostics method, large-area tracking detectors are needed to provide a necessary statistical accuracy for each angular direction within the device aperture. The registration system should not only provide localization of the anomaly but also trace its further propagation. This imposes quite high requirements to the system of primary analysis, formation and presentation of the obtained physical information in real time.

The main advantage of wide-aperture muon hodoscopes compared to multidirectional muon telescopes is the possibility of reconstruction in real time of the track of each muon arriving from any direction of the upper hemisphere. To provide acceptable flows of processed and accumulated information, a matrix method of representing experimental data has been applied, which is described below.

## Experimental setup

Muon hodoscope (MH) URAGAN (Chernov et al. 2005; Barbashina et al. 2008), a wide-aperture coordinate-tracking detector which detects in a real-time mode the muon flux at the Earth's surface in a wide range of zenith angles (0–80°) with a high angular resolution (~1°), was constructed in the Scientific and Educational

Centre NEVOD, MEPhI. The main objective of the facility is the study of variations of the angular distribution of the muon flux caused by various atmospheric and extra-atmospheric processes. The URAGAN consists of four independent supermodules. Each supermodule (SM) (**Figure 1**) represents an assembly of eight planes of streamer tube chambers blown with a gas mixture  $\text{Ar} + \text{CO}_2 + \text{n-pentane}$ . Sixteen gas discharge tubes with size  $9 \times 9 \times 3500 \text{ mm}^3$  and resistive cathode coating operated in a limited streamer mode are enclosed in a single plastic container. Each plane contains 320 tubes equipped with an external X-Y-strips coordinate read-out system. Sensitive area of one SM is  $\sim 11.5 \text{ m}^2$ . Trigger condition of the event detection is the coincidence of signals from the strips of 4 or more X-strip planes within the time gate of 250 ns. The scheme of the muon detection in the SM is shown in **Figure 2**.

### Data format

As described in the article (Yashin et al. 2015a), the track parameters (two projection angles) are reconstructed in a real-time mode by means of the software which is based on the histogramming technique in each projection plane XZ and YZ and are stored in a two-dimensional data matrix over one-minute time



**Figure 1:** The muon hodoscope URAGAN. In the foreground, one of the supermodules is seen. On the left and at the background the other three SM are located.

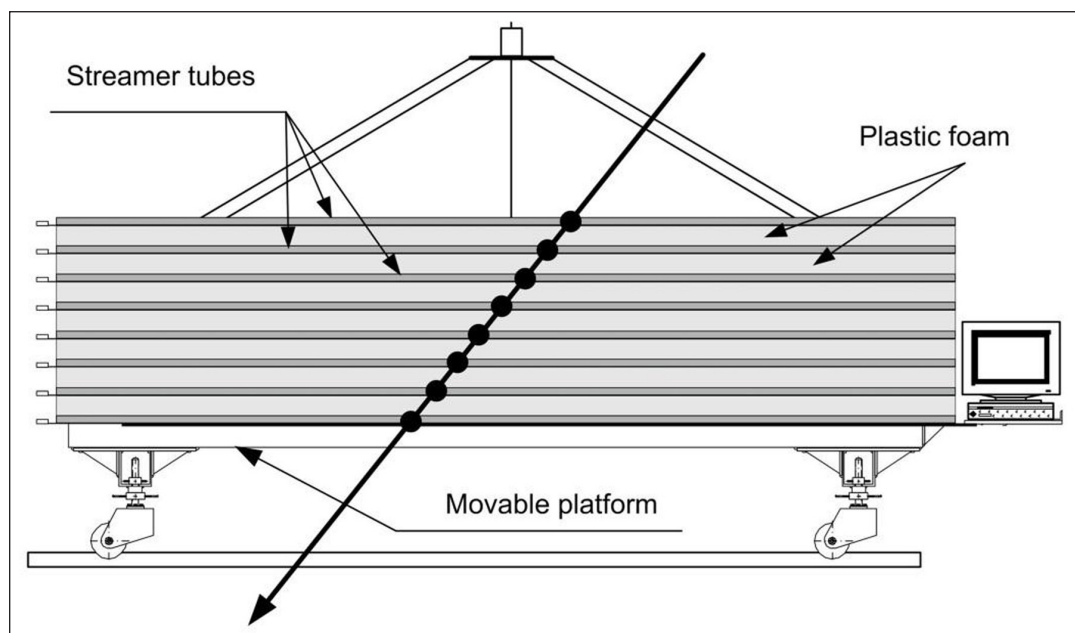


**Figure 2:** Scheme of single particle detection in the SM.

interval. This data array is a “muon snapshot” of the upper hemisphere (limited by the detector aperture) acquired with a one-minute exposure. The monitoring data include results of testing of serial data readout circuits, measurements of the SM plane noise rate, hit channel maps and estimates of the efficiency of particle track detection by the planes.

The angular distribution of the tracks for 1 minute measurement interval is stored in the forms of three types of matrices with dimensions of  $90 \times 90$  cells: zenith and azimuth angles  $(\theta, \varphi)$   $M_a \equiv [\theta_i, \varphi_j]$ ; in projection angles  $(\theta_x, \theta_y)$ ,  $M_{pa} \equiv [\theta_{xi}, \theta_{yj}]$ ; in tangents of projection angles  $(\text{tg}\theta_x, \text{tg}\theta_y)$ ;  $M_{tg} \equiv [\text{tg}\theta_{xi}, \text{tg}\theta_{yj}]$ . Different types of matrices are used for solution of different tasks. The matrix  $M_a$  is used to study angular characteristics of the muon flux (for example, the anisotropy and energy dependences of the muon flux during Forbush decreases). The  $M_{tg}$  matrix is used to construct images-muonographs (Yashin et al. 2015a) (projection on the muon generation layer in the atmosphere to study thunderstorm events or projection on a magnetopause to study geoeffective events during the disturbances on the Sun). The  $M_{pa}$  matrix is used to more accurately study the effects in the directions close to the vertical (for example, Ground Level Enhancement (GLE) analysis).

Every matrix contains the angular distribution of muons measured during 1-minute interval. The sequence of such matrices gives a unique possibility to study the temporal changes of muon angular distributions. Depending on the analysis to be performed, matrices can be combined in different time intervals  $\Delta t$ . For example, for the analysis of muon flux variations of heliospheric origin, the matrix data summed during  $\Delta t = 1$  h may be used. For the study the dynamics of rapidly developing atmospheric processes that cause variations in the intensity of muons, five-minute matrices are analyzed.

### Real-time data processing

Data processing is carried out in a real-time mode. Time series of averaged over 1- and 60-min intervals atmospheric pressure, counting rates of reconstructed tracks (without the barometric and temperature corrections), and “live”-times for every supermodule are formed. These series are stored in 1- and 60-min daily files in a text format. At the beginning of each hour, an additional processing is carried out, for which the data of three SM (SM1, SM3 and SM4) are used, while SM2 is used mainly for methodical and calibration purposes. The purpose of data processing procedures is the creation of time series of the angular distribution of muons and of parameters of the counting rate analysis. Results of additional processing are:

- time series of characteristics of angular distributions of 60-minute matrices  $M_{a,1h}$ ;
- time series of characteristics of the angular distributions of 60-minute matrices  $M_{tg,1h}$ ;
- time series of results of the wavelet analysis of 10- and 60-minute counting rates and characteristics of zenith-angular distributions;
- image files of 60-minute matrices  $M_{tg,1h}$  of variations in the angular distributions in the East-North (local geographic) and GSE (Geocentric Solar Ecliptic) coordinate systems;
- image files of obtained time-series graphs.

Images of time series graphs and of matrices of variations of the angular distribution are presented at the web pages (Yashin et al. 2015b):

- “Integral intensity mode” and “Hodoscopic mode”: [http://nevod.mephi.ru/uragan\\_data.htm](http://nevod.mephi.ru/uragan_data.htm);
- “Heliosphere” (60-minute muon flux variation analysis): <http://nevod.mephi.ru/English/heliosphere.php>;
- “Wavelets of URAGAN data”: <http://nevod.mephi.ru/English/wavurg.htm>.

### Corrections for atmospheric effects

Changes of the atmospheric conditions modulate the muon flux at the Earth’s surface, and variations of the extra-atmospheric origin are of the same order. Therefore, to study the extra-terrestrial effects it is necessary first to correct all the matrices for the main atmospheric effects, barometric and temperature ones.

Barometric effect is the anti-correlation of cosmic ray intensity with the pressure at the observation level. Temperature effect is caused by changes of the temperature at all altitudes of the atmosphere. Corrected angular matrix  $M^{\text{corr}}(\theta, \varphi, t, \Delta t)$  can be calculated in a following way:

$$M^{\text{corr}}(\theta, \varphi, t, \Delta t) = M(\theta, \varphi, t, \Delta t) + \Delta M_p(\theta, t, \Delta t) + \Delta M_T(\theta, t, \Delta t), \quad (1)$$

where  $\theta$  and  $\varphi$  are zenith and azimuth angles for matrix cell centers;  $M(\theta, \varphi)$  is the number of reconstructed events in a cell  $(\theta, \varphi)$  of the matrix  $M$ ;  $t$  is the time of the beginning and  $\Delta t$  is the time interval of the matrix accumulation;  $\Delta M_T$  and  $\Delta M_P$  are corrections for temperature and barometric effects. Barometric correction is calculated as

$$\Delta M_P(\theta) = B(\theta) \cdot (P - P_0), \quad (2)$$

where  $P$  is the current pressure at registration level,  $P_0 = 993$  mbar is the averaged over a long time period pressure at the registration level,  $B(\theta)$  are barometric coefficients. Temperature correction is

$$\Delta M_T(\theta) = M_0(\theta) \cdot \sum_i W_T(h_i, \theta) \Delta T(h_i) \Delta h_i / 100\%, \quad (3)$$

where  $M_0(\theta)$  is the over a long period averaged number of reconstructed events for zenith angle  $\theta$ ,  $W_T(h, \theta)$  are differential in altitude temperature coefficients (DTC) (Dmitrieva et al. 2011),  $\Delta T(h) = T_{SMA}(h) - T(h)$  is the change of the temperature,  $h$  is the atmospheric depth,  $\Delta h = 0.05$  atm,  $T(h)$  is the current temperature profile of the atmosphere,  $T_{SMA}(h)$  is the temperature profile for the standard model of the atmosphere. In calculations, a six-layer stationary spherical model of the atmosphere is used, contributions of both pions and kaons are taken into account. Also for muons, the relation between specific energy loss and muon energy. The altitude above sea level and threshold energies of the muon hodoscope URAGAN have been taken into account.

Information about the temperature profile of the atmosphere can be obtained from the following sources (Dmitrieva et al. 2015):

1. Information from direct measurements of air temperature with the help of meteorological balloon flights. For example, for URAGAN data correction the information from the Central Aerological Observatory (Russia, Dolgoprudny) is used. Usually temperature profile is measured by meteorological balloons two times a day, at 00:00 and 12:00 UT. Unfortunately, sometimes launches of meteorological balloons are not carried out, or balloons do not raise high enough.
2. The alternative sources are weather forecasting models of the atmosphere. One of them is the numerical forecasting model of the atmosphere GDAS (The Global Data Assimilation System). GDAS output data are available 8 times a day for the whole globe (1 degree latitude-longitude grid) and for 23 constant pressure levels (from 1000 to 20 mbar). Retrospective archive data (since 2005) are in the open access (NOAA Air Resources Laboratory <http://ready.arl.noaa.gov/gdas1.php>).

In **Figure 3**, 10-minute average counting rates of the URAGAN hodoscope without and with corrections for meteorological effects are shown for a one year period. Barometric coefficients for URAGAN slightly depend on the zenith angle and are about  $\sim 0.18\%$ /mbar. After correction for barometric effect, annual variations caused by the temperature effect ( $\sim 8\%$ ) become well visible. After correction for the temperature effect, variations caused by extra-atmospheric processes appear.

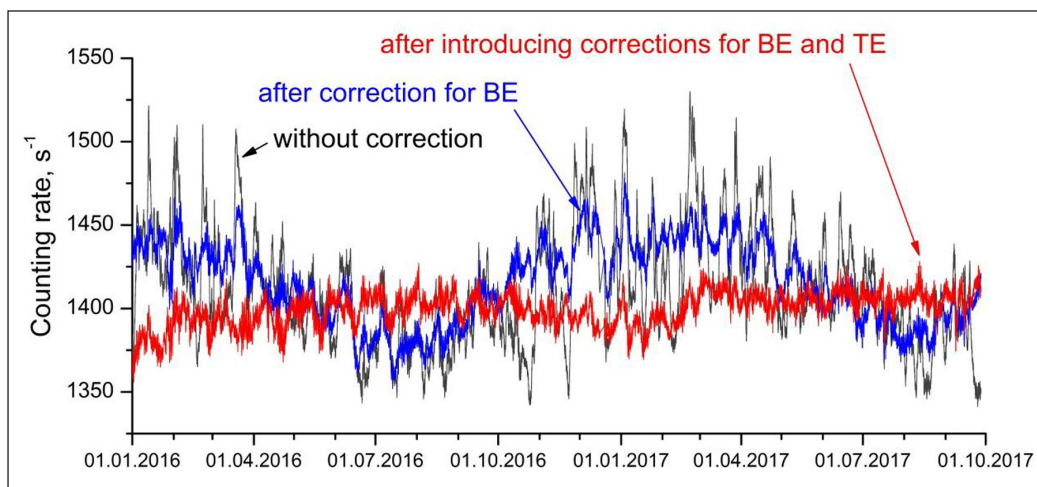


**Figure 3:** 10-minute average counting rates of the URAGAN hodoscope without and with corrections for meteorological effects.



## Changes of local anisotropy of the muon flux during heliospheric disturbances

For the study of the response of muon flux variations registered by the muon hodoscope URAGAN, the local anisotropy vector  $\mathbf{A}$ , one of the main characteristics of the angular distribution of muon flux, which is the sum of unit vectors with directions of reconstructed tracks in individual events normalized to the total number of muons was used. The local anisotropy vector  $\mathbf{A}$  indicates the average arrival direction of muons and is close to the vertical. For the study of its deviations from the average direction, a relative anisotropy vector that is the difference between the current value of the vector and the average anisotropy vector calculated over a long period of time is used:  $\mathbf{r} = \mathbf{A} - \langle \mathbf{A} \rangle$ . The length of the horizontal projection of the relative anisotropy vector characterizes the “side influence” on the angular distribution of the muon flux and is given by:  $r_h = \sqrt{r_x^2 + r_y^2}$ . For the convenience of comparison of different events, its value is expressed in units of the RMS deviation ( $\sigma$ ).

The  $r_h$  parameter is sensitive to the changes in the interplanetary magnetic field induced by the active processes on the Sun. The variations of the horizontal projection of the vector of local anisotropy can be used to identify the time intervals of the increased anisotropy, which are observed during the passage of various irregularities in the solar wind and the interplanetary magnetic field in the Earth’s vicinity. Study of the muon flux anisotropy during periods of heliospheric disturbances is based on the comparison of data of satellite detectors and muon hodoscope URAGAN. To estimate the state of the interplanetary space, the values of the modulus of the magnetic induction vector  $B$  and the solar wind velocity  $V_{sw}$  were used in the work. To estimate the state of the magnetosphere, the values of the geomagnetic activity index  $K_p$  were used (OMNI Database <https://omniweb.gsfc.nasa.gov/>). **Figure 4** shows changes in the parameters  $B$ ,  $V_{sw}$ ,  $K_p$ -index, counting rate  $N$  (normalized to one SM) and the parameter of the local anisotropy  $r_h / \sigma_{r_h}$  according to URAGAN for the period from September 9 to October 10, 2016 (Astapov et al. 2015).

The horizontal lines in the graphs indicate the boundaries for the determination of perturbations in the interplanetary space ( $B$ ,  $V_{sw}$ ), the Earth’s magnetosphere ( $K_p$ ) and the cosmic-ray muon flux ( $r_h / \sigma_{r_h}$ ). The vertical line marks the coronal mass ejection (CME) recorded by the coronagraph from the STEREO satellite on September 15, 2016 at 00:23 UT with an average speed of 625 km/s.

As can be seen from the upper graphs, the ejection affected the interplanetary magnetic field. The increase in the values of magnetic induction began on September 18, the maximum was reached on September 19 and amounted to 18.9 nT. There was also a disturbance in the values of the solar wind speed, its maximum occurred on September 20 and amounted to 727 km/s. The perturbations of these parameters in the interplanetary space were confirmed by the geomagnetic activity index  $K_p = 4$ .

The response of the muon hodoscope to the CME was visible one day after ejection. Three distinct peaks were repeated at regular intervals once per day and are clearly seen on the last graph. The projection of the

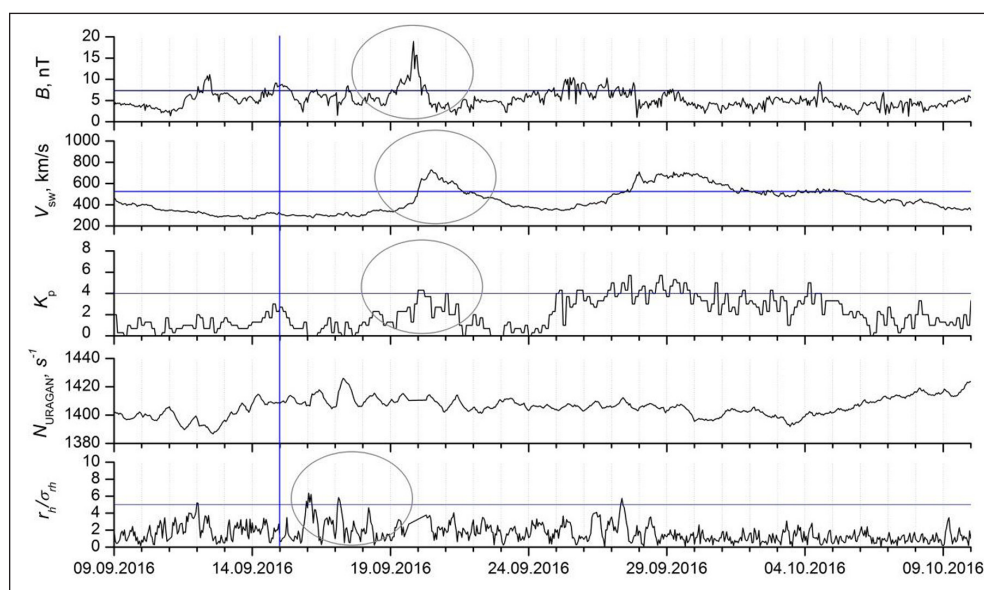


**Figure 4:** Temporal changes in parameters  $B$ ,  $V_{sw}$ ,  $K_p$ -index, counting rate and the parameter of the local anisotropy according to URAGAN for the period from September 9 to October 10, 2016.

relative anisotropy vector  $r_h$  in  $\sigma_h$  units reached a maximum value on September 16 at 01:00,  $r_h / \sigma_h = 6.4$ . The second peak was observed on September 17 at 03:00 and amounted to  $r_h / \sigma_h = 5.8$ , which in both cases corresponded to a perturbation of the local anisotropy of the muon flux.

## Conclusions

Muon hodoscope is a cosmic-ray detector designed to study the relations between the spatial and temporal variations of the cosmic ray muon flux and various dynamic processes in the heliosphere and magnetosphere of the Earth. Development of the URAGAN hodoscope offers a chance to attain a new qualitative level in investigating and monitoring processes in the near-Earth space, in particular those of a dangerous character. For implementation of fast and effective primary processing of a large flow of multidimensional information from the muon hodoscope URAGAN in a real time, a matrix approach to data representation was proposed and realized. Characteristics of the anisotropy of the angular distribution of muons provide a convenient tool for the study of the processes of cosmic ray flux modulation of atmospheric and extra-terrestrial origin.

## Acknowledgements

This work was performed in the Scientific and Educational Center NEVOD with the state financial support provided by the Russian Scientific Foundation (RSF), project No. 17-17-01215 "Creation of a method for early diagnostics of geomagnetic storms based on digital processing of time series of observational matrices of a muon hodoscope".

## Competing Interests

The authors have no competing interests to declare.

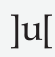
## References

- Astapov, II, Barbashina, NS, Dmitrieva, AN**, et al. 2013. Study of heliospheric disturbances on the basis of cosmic ray muon flux anisotropy. *J. Phys.: Conf. Ser.*, 409: 012196. DOI: <https://doi.org/10.1088/1742-6596/409/1/012196>
- Astapov, II, Barbashina, NS, Dmitrieva, AN**, et al. 2015. Local anisotropy of muon flux – the basis of the method of muon diagnostics of extra-terrestrial space. *Advances in Space Research*, 56: 2713–2718. DOI: <https://doi.org/10.1016/j.asr.2015.05.039>
- Barbashina, NS, Kokoulin, RP, Kompaniets, KG**, et al. 2008. The URAGAN wide-aperture large-area muon hodoscope. *Instrum. Exp. Tech.*, 51: 180–186. DOI: <https://doi.org/10.1134/S002044120802005X>
- Central Aerological Observatory**. Russia, Dolgoprudny. <http://www.aerology.org/> [Accessed, December, 2017].
- Chernov, DV, Barbashina, NS, Mannocchi, G**, et al. 2005. Experimental setup for muon diagnostics of the Earth's atmosphere and magnetosphere (the URAGAN project). *Proceedings of the 29th International Cosmic Ray Conference*, 2: 457–460.
- Dmitrieva, AN**, et al. 2011. Corrections for temperature effect for ground-based muon hodosopes. *Astroparticle Physics* 34(6): 401–411. DOI: <https://doi.org/10.1016/j.astropartphys.2010.10.013>
- Dmitrieva, AN, Ampilogov, NV, Astapov, II**, et al. 2015. Temperature effect corrections for URAGAN based on CAO, GDAS, NOAA data. *Journal of Physics: Conference Series*, 632: 012054. DOI: <https://doi.org/10.1088/1742-6596/632/1/012054>
- NOAA Air Resources Laboratory**. <http://ready.arl.noaa.gov/gdas1.php> [Accessed, December, 2017].
- OMNI Database**. <https://omniweb.gsfc.nasa.gov/> [Accessed, December, 2017].
- Shutenko, VV, Barbashina, NS, Kompaniets, KG**, et al. 2009. Observation of heliospheric disturbances in the muon component of cosmic rays. *Bulletin of the Russian Academy of Sciences: Physics*, 73(3): 347–349. DOI: <https://doi.org/10.3103/S1062873809030204>
- Yashin, II, Astapov, II, Barbashina, NS**, et al. 2015b. Real-time experimental data of the muon hodoscope URAGAN accessible in www. *Journal of Physics: Conference Series*, 632: 012086. DOI: <https://doi.org/10.1088/1742-6596/632/1/012086>
- Yashin, II, Astapov, II, Kokoulin, RP**, et al. 2015a. Real-time data of muon hodoscope URAGAN. *Advances in Space Research*, 56: 2693–2705. DOI: <https://doi.org/10.1016/j.asr.2015.06.003>

**How to cite this article:** Kovylyayeva, A, Astapov, I, Dmitrieva, A, Borog, V, Osetrova, N and Yashin, I. 2020. Experimental Data of Muon Hodoscope URAGAN for Investigations of Geoeffective Processes in the Heliosphere. *Data Science Journal*, 19: 11, pp.1–7. DOI: <https://doi.org/10.5334/dsj-2020-011>

**Submitted:** 07 December 2017    **Accepted:** 27 January 2020    **Published:** 16 March 2020

**Copyright:** © 2020 The Author(s). This is an open-access article distributed under the terms of the Creative Commons Attribution 4.0 International License (CC-BY 4.0), which permits unrestricted use, distribution, and reproduction in any medium, provided the original author and source are credited. See <http://creativecommons.org/licenses/by/4.0/>.

 *Data Science Journal* is a peer-reviewed open access journal published by Ubiquity Press.

**OPEN ACCESS** 